



ELSEVIER

Journal of Organometallic Chemistry 657 (2002) 205–216

Journal
of Organo
metallic
Chemistry

www.elsevier.com/locate/jorgchem

Azanonaborane-pyridine derivatives [(R'C₅H₄N)B₈H₁₁NHR'']: synthesis, structure and some molecular-orbital calculations

Claudia Bauer^a, Detlef Gabel^a, Tobias Borrmann^a, John D. Kennedy^b,
Colin A. Kilner^b, Mark Thornton-Pett^b, Udo Dörfler^{a,*}

^a Department of Chemistry, University of Bremen, P.O. Box 330 440, 28334 Bremen, Germany

^b Department of Chemistry, University of Leeds, Leeds, England LS2 9JT, UK

Received 15 October 2001; accepted 22 March 2002

Abstract

The molecular structure of *hypho*-type [(RNH₂)B₈H₁₁NHR] is based on a {B₈} cluster with one nitrogen bridge and one *exo* amine ligand. In general these azanonaboranes are synthesized by the reaction of [B₉H₁₃(SMe₂)] with primary amines. Modifications of these azanonaboranes are possible by ligand-exchange reactions. Necessary conditions for ligand-exchange reactions of the azanonaboranes [(RNH₂)B₈H₁₁NHR], in which the *exo*-{NH₂R} group is replaced by other nitrogen-donor ligands, are reported. The nitrogen-donor ligands that have been examined include primary, secondary and tertiary amines as well as a series of substituted pyridines. The structures of the pyridine-containing azanonaboranes [(C₅H₅N)B₈H₁₁NHR] where R = methyl, ethyl, *iso*propyl or tertiary butyl, have been determined crystallographically, and are compared with the aliphatic azanonaboranes [(RNH₂)B₈H₁₁NHR]. The reactions of the various [(RNH₂)B₈H₁₁NHR] species with pyridine or the substituted pyridines give coloured products, contrasting with the colourless nature of the starting alkylamine species. The electronic interaction between the {B₈} *hypho*-type unit and the bonded pyridine units has been investigated by UV–vis spectroscopy and by AM-1 molecular-orbital calculations. © 2002 Elsevier Science B.V. All rights reserved.

Keywords: *Hypho* cluster; Azanonaborane; N ligands; X-ray crystal structure; MO calculations

1. Introduction

The azanonaboranes [(RNH₂)B₈H₁₁NHR] are available via simple three- or four-step reactions from commercially available *nido*-decaborane(14), B₁₀H₁₄. [(EtNH₂)B₈H₁₁NHET] was the first compound of this family to be reported [1,2]. [(EtNH₂)B₈H₁₁NHET] was first synthesized in 1962 by the reaction of [B₉H₁₃(SMe₂)] with NH₂Et [1], and the determination of its structure and thence unequivocal constitution followed in 1963 [2]. Some time later, the results of NMR-spectroscopy were taken to suggest that the eight-boron core cluster of this compound could be defined as being in a *hypho* category [3]. Thus, its molecular structure is based on a {B₈} cluster [2] of interesting *hypho*-type eight-vertex character [3] that has two

amine-type residues attached to it, viz. one amino group {NHET} in a boron–boron bridging position, and one ligand unit NH₂Et in an *exo* terminal position (Fig. 1). The description of the eight-vertex borane cluster of [(RNH₂)B₈H₁₁NHR] in terms of *hypho* character can be based on the Williams–Wade formalism, often described as ‘Wade’s rules’ [4]. This formalism classifies the relationship between the skeletal structures of boranes and the numbers of electron pairs that they contain. Thus, a species with *n* skeletal atoms will adopt a *hypho* structure if held together by (*n*+4) electron pairs. In the [(RNH₂)B₈H₁₁NHR] cluster system the *exo* amine NH₂R is a two-electron-donor ligand to the eight-boron central cluster, whereas the {NHR} group is an electron-precise moiety that is formally attached to two skeletal boron atoms via one normal covalent bond and one dative bond. The {NHR} unit thereby gives three electrons to the cage. The boron cage itself provides nineteen cluster-bonding electrons to the framework. Together with the total of five electrons from the two

* Corresponding author. Tel.: +49-421-218-2200; fax: +49-421-218-2871.

E-mail address: doerfler@chemie.uni-bremen.de (U. Dörfler).

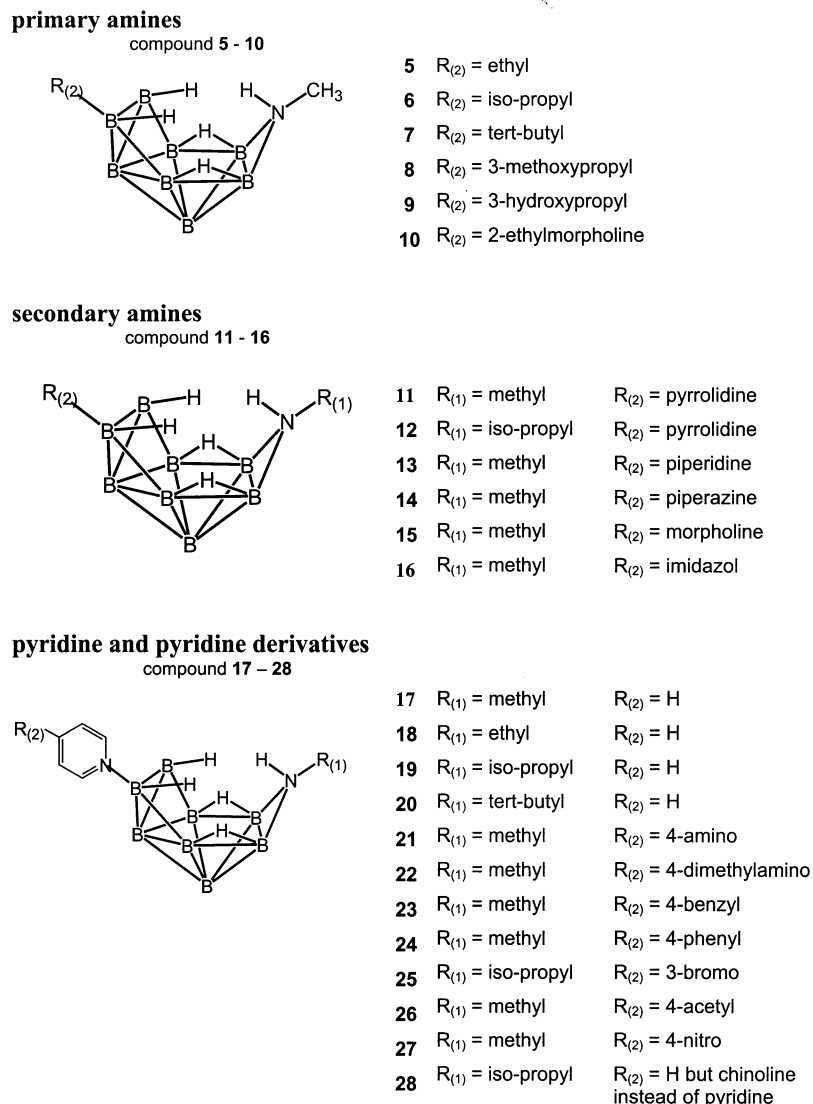


Fig. 1. Generalised schematic structure of compounds 5–28 of the $[(RNH_2)B_8H_{11}NHR]$ family (BH *exo* hydrogen atoms are omitted for clarity). The compounds may be regarded as *hypho*-type eight-vertex $\{B_8\}$ cluster species, or as *arachno*-type nine-vertex $\{B_8N\}$ cluster species.

nitrogen centres, 24 electrons (12 electron pairs) are, therefore, available for the eight skeletal atoms. Consequently, the $[(RNH_2)B_8H_{11}NHR]$ species fulfil the conditions for being an eight-vertex member of the *hypho* cluster family. In nine-vertex azanonaborane terms, i.e. by inclusion of the bridging nitrogen atom of the $\{NHR\}$ grouping as a cluster constituent, then the species will have nine-vertex *arachno* character [3], with a $\{B_8N\}$ skeletal geometry that mimics that of the arachno nine-vertex binary borane $n-B_9H_{15}$.

Subsequently, it was shown that this route into this system is not limited to the reaction of $[B_9H_{13}(SMe_2)]$ with NH_2Et [5,6], but that other primary amines NH_2R , such as *iso*-propylamine, *n*-butylamine, *tert*-butylamine [5] and methylamine [6] also generate their corresponding $[(RNH_2)B_8H_{11}NHR]$ species. In some cases, it is also possible to use secondary amines, as in the use of NH_2Et_2

to give $[(Et_2NH)B_8H_{11}NEt_2]$ [6], but in this case the yield is not very high. In addition to these direct syntheses from $[B_9H_{13}(SMe_2)]$, a second route to secondary-amine derivatives is via the modification of the nitrogen-containing groups by N-deprotonation of the $[(RNH_2)B_8H_{11}NHR]$ system and subsequent N-alkylation [6].

Compounds of this family constitute interesting entries into azacarbaborane [7] and azametallaborane chemistries [8,9] and also have interesting potential for use as boron carriers for boron neutron-capture therapy [10]. In order further to facilitate the development of this new azanonaborane science, we have been investigating other possible routes to and among these species. In this context, we here report a ligand-exchange reaction in which the *exo*- NH_2R ligand is replaced by other nitrogen-donor ligands, both aliphatic and aromatic.

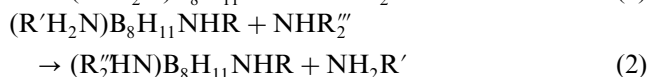
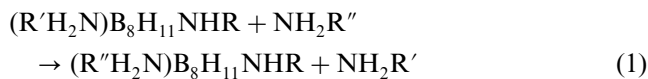
During the course of our initial experiments, reactions carried out with unsubstituted pyridine NC_5H_5 as donor ligand gave a bright yellow $[(\text{C}_5\text{H}_5\text{N})\text{B}_8\text{H}_{11}\text{NHEt}]$ product, contrasting with the colourless nature of the starting alkylamine species. In view of this, a series of substituted pyridines $\text{R}'\text{C}_5\text{H}_4\text{N}$, where R' is both electron-donating and electron-withdrawing, e.g. 4- NH_2 , 4- CHO and 3- Br , have also been used in the ligand-exchange reactions with species $[(\text{RNH}_2)\text{B}_8\text{H}_{11}\text{NHR}]$, in order to investigate for variety of colour-change differences in the products $[(\text{R}'\text{C}_5\text{H}_4\text{N})\text{B}_8\text{H}_{11}\text{NHR}]$. Such colourations suggest that there is an electronic interaction between the $\{\text{B}_8\}$ *hypho*-type unit and the bonded pyridine units. This phenomenon may be related to that found for other borane-pyridine complexes, particularly those of the [6,9-*L*₂-*arachno*- $\text{B}_{10}\text{H}_{12}$] constitution [11–13].

Thus, we report here on the synthesis and structure of several new members of this family of azanonaboranes, and also, with the pyridine and substituted pyridine species, compare these experimental results with the calculated structures and UV–vis spectra obtained from semi-empirical AM-1 molecular-orbital calculations. One ultimate calculational target here is to develop a qualitative molecular-orbital model to explain the UV–vis spectra of these azanonaborane–pyridine derivatives in terms of a dependence on the substituents on the pyridine ring. In this regard, we also here compare conclusions regarding the electronic interaction between the pyridine moieties and the *hypho*-type $\{\text{B}_8\}$ clusters in compounds of the $[(\text{R}'\text{C}_5\text{H}_4\text{N})\text{B}_8\text{H}_{11}\text{NHR}]$ series with those previously reported [11–13] for the ten-vertex [6,9- $(\text{R}'\text{C}_5\text{H}_4\text{N})_2$ -*arachno*- $\text{B}_{10}\text{H}_{12}$] cluster system.

2. Results and discussion

2.1. Preparation

We have found that the exchange of the *exo* amine ligand $\text{NR}'\text{H}_2$ for another amine $\text{NH}_2\text{R}''$ or NHR'' (equation 1 and 2, respectively) is a convenient route for the formation of new N-substituted members of this azanonaborane family, of general formulations $[(\text{R}'\text{NH}_2)\text{B}_8\text{H}_{11}\text{NHR}]$ or $[(\text{R}_2''\text{HN})\text{B}_8\text{H}_{11}\text{NHR}]$, respectively.



In initial experiments, we investigated the dependence of the ligand-exchange reaction on the solvent, using $[(\text{EtNH}_2)\text{B}_8\text{H}_{11}\text{NHEt}]$ and pyridine as the test system. The result of this investigation is that the necessary

temperatures have to be no less than 80 °C but not higher than 150 °C. Decomposition occurs at 150 °C and above. The aromatic solvents benzene, toluene and xylene can be used, but attempts using the non-polar non-aromatic solvent hexane were not productive. In terms of more polar solvents, the ligand-exchange reaction can be carried out in 1,4-dioxane, whereas use of tetrahydrofuran was not successful, presumably because of its lower boiling point (b.p.). Polar solvents with hydroxyl groups, e.g. ethanol and propanol, cannot be used for the ligand-exchange reaction because they decompose the azanonaborane at these temperatures. No reaction was observed in the polar aprotic solvent acetonitrile, even though the b.p. is in principle high enough.

Following this initial survey, we adopted benzene as solvent of choice for subsequent investigation, and we thence investigated primary, secondary and tertiary aliphatic amines, together with pyridine and substituted pyridines, for use in the ligand-exchange reaction. Successful syntheses were obtained with primary amines that contained either non-polar residues, or polar residues distal to the amine site, to yield $[(\text{EtNH}_2)\text{B}_8\text{H}_{11}\text{NHMe}]$ **5**, $[(^{i\text{so}}\text{PrNH}_2)\text{B}_8\text{H}_{11}\text{NHMe}]$ **6**, $[(^{t\text{er}}\text{BuNH}_2)\text{B}_8\text{H}_{11}\text{NHMe}]$ **7**, $[\{\text{MeO}(\text{CH}_2)_3\text{NH}_2\}\text{B}_8\text{H}_{11}\text{NHMe}]$ **8**, $[\{\text{HO}(\text{CH}_2)_3\text{NH}_2\}\text{B}_8\text{H}_{11}\text{NHMe}]$ **9**, and $[\{\text{OC}_4\text{H}_8\text{NH}(\text{CH}_2)_2\text{NH}_2\}\text{B}_8\text{H}_{11}\text{NHMe}]$ **10**. However, the reaction did not proceed with the aromatic amine aniline under corresponding conditions. Primary amines with adjacent polar groups, such as 2-methoxyethylamine, 2,2-diethoxyethylamine or *N*-acetylenylendiamine, similarly did not undergo the ligand-exchange reactions. Empirically, for these substituted primary amines, we found that there must be more than two $\{\text{CH}_2\}$ groups between the $\{\text{NH}_2\}$ residue and the polar functional group in the amine.

Diethylamine and diallylamine, viz. secondary amines with non-polar residues, also react with $[(\text{RNH}_2)\text{B}_8\text{H}_{11}\text{NHR}]$ to yield the corresponding products $[(\text{R}_2\text{NH})\text{B}_8\text{H}_{11}\text{NHR}]$ [6]. Use of non-aromatic cyclic secondary amines also conveniently gives their corresponding products. Both five-membered-ring species, as with pyrrolidine in $[(\text{C}_4\text{H}_8\text{NH})\text{B}_8\text{H}_{11}\text{NHMe}]$ **11** and $[(\text{C}_4\text{H}_8\text{NH})\text{B}_8\text{H}_{11}\text{NH}^{i\text{so}}\text{Pr}]$ **12**, and six-membered-ring species, as in the piperidine compound $[(\text{C}_5\text{H}_{10}\text{NH})\text{B}_8\text{H}_{11}\text{NHMe}]$ **13**, can be prepared. Here it is of interest to note that differences in the $\{\text{NHR}\}$ residue that is bonded to the bridging nitrogen atom also do not significantly change the reactivity, with comparable yields being obtained for the $\{\text{NHMe}\}$ compound **11** and the $\{\text{NH}^{i\text{so}}\text{Pr}\}$ compound **12**. The reaction also proceeds when there are ring heteroatoms in the cyclic aliphatic amine, as with a nitrogen atom, as in $[(\text{NHC}_4\text{H}_8\text{NH})\text{B}_8\text{H}_{11}\text{NH}^{i\text{so}}\text{Pr}]$ **14**, or an oxygen atom, as in $[(\text{OC}_4\text{H}_8\text{NH})\text{B}_8\text{H}_{11}\text{NHCH}_3]$ **15**. As with the primary amines as discussed in the previous paragraph,

the ligand-exchange reaction does not occur with some examples of substituted secondary amines in which there is only a short carbon chain between the substituent group and the amine unit. These examples are diethanolamine and *N,N,N'*-trimethylethylenediamine. Pyrrole as an aromatic amine does not undergo the ligand-exchange reaction, presumably because the nominally isolated electron pair of the nitrogen atom is part of the aromatic π -electron system. The reaction with imidazole does, however, occur, presumably now because its character is more basic than that of pyrrole: imidazole contains two nitrogen atoms and only one of the nitrogen electron pairs is needed for the aromatic π -electron system. As a model for tertiary amines, reactions were also tried with triethylamine, but no exchange reaction occurred under our conditions, presumably because of inhibitory steric effects.

The ligand exchange also occurs readily with pyridine to yield the yellow product $[(C_5H_5N)B_8H_{11}NHMe]$ **17**. We thence investigated for pyridine derivatives with a range of electron-donating and electron-accepting substituents, firstly to establish whether the exchange also occurs at extremes of donating and accepting substituent effect, and secondly to examine for differences of colour in the products. The substituted pyridines used were 4-dimethylaminopyridine, 4-aminopyridine, 4-benzylpyridine, 4-phenylpyridine, 3-bromopyridine, 4-acetylpyridine, 4-nitropyridine and chinoline. These experiments resulted in the formation of $[(C_5H_5N)B_8H_{11}NHMe]$ **17**, $[(C_5H_5N)B_8H_{11}NHEt]$ **18**, $[(C_5H_5N)B_8H_{11}NH^{iso}Pr]$ **19**, $[(C_5H_5N)B_8H_{11}NH^{ter}Bu]$ **20**, $[(4-NH_2C_5H_4N)B_8H_{11}NHMe]$ **21**, $[(4-NMe_2-C_5H_4N)B_8H_{11}NHMe]$ **22**, $[(4-PhCH_2-C_5H_4N)B_8H_{11}NHMe]$ **23**, $[(4-Ph-C_5H_4N)B_8H_{11}NHMe]$ **24**, $[(3-Br-C_5H_4N)B_8H_{11}NH^{iso}Pr]$ **25**, $[(4-MeCO-C_5H_4N)B_8H_{11}NHMe]$ **26** and $[(4-NO_2-C_5H_4N)B_8H_{11}NHMe]$ **27**. Both reactivity and yield were both very similar for the pyridines with both donor or acceptor substituents, and there was similarly little variation between 3-substituted analogues and 4-substituted analogues. In all such cases the exchange reaction worked very well. However, 2-substitution is presumably sterically inhibitory, as we observed no reaction when either 2,6-dimethylpyridine, or 2,2'-dithiopyridine, or acridine, were used.

2.2. Structural study

The four pyridine compounds $[(C_5H_5N)B_8H_{11}NHMe]$ **17**, $[(C_5H_5N)B_8H_{11}NHEt]$ **18**, $[(C_5H_5N)B_8H_{11}NH^{iso}Pr]$ **19** and $[(C_5H_5N)B_8H_{11}NH^{ter}Bu]$ **20**, were examined by single-crystal X-ray diffraction analysis (Fig. 2, Fig. 3, Fig. 4 and Fig. 5).

The results readily confirmed the identities of the compounds, and were consistent with the results of NMR spectroscopy (for details see Section 3), confirming that the crystals selected were representative of the

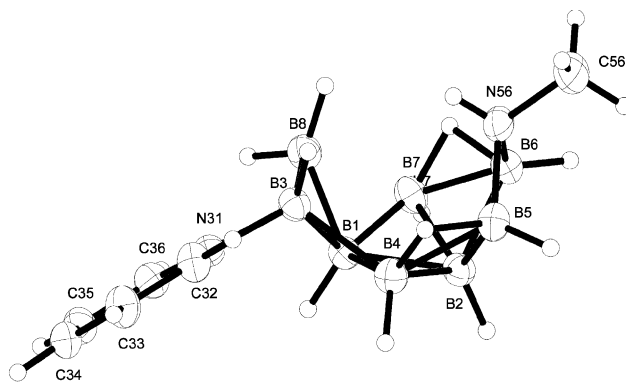


Fig. 2. A drawing of the crystallographically determined molecular structure of $[(C_5H_5N)B_8H_{11}NHMe]$ **17**, with thermal ellipsoids of non-hydrogen atoms shown at 50% probability. For clarity hydrogen atoms are drawn as circles with an arbitrary small radius.

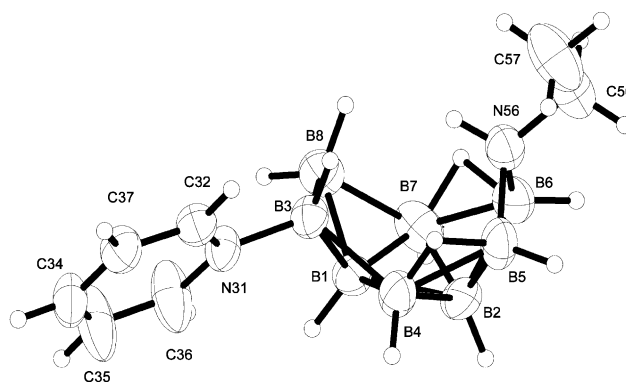


Fig. 3. A drawing of the crystallographically determined molecular structure of one of the two independent molecules of $[(C_5H_5N)B_8H_{11}NHEt]$ **18**, with thermal ellipsoids of non-hydrogen atoms shown at 50% probability. For clarity hydrogen atoms are drawn as circles with an arbitrary small radius.

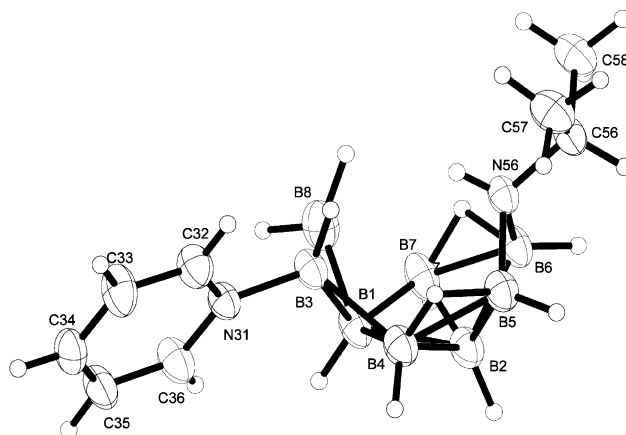


Fig. 4. A drawing of the crystallographically determined molecular structure of $[(C_5H_5N)B_8H_{11}NH^{iso}Pr]$ **19**, with thermal ellipsoids of non-hydrogen atoms shown at 50% probability. For clarity hydrogen atoms are drawn as circles with an arbitrary small radius.

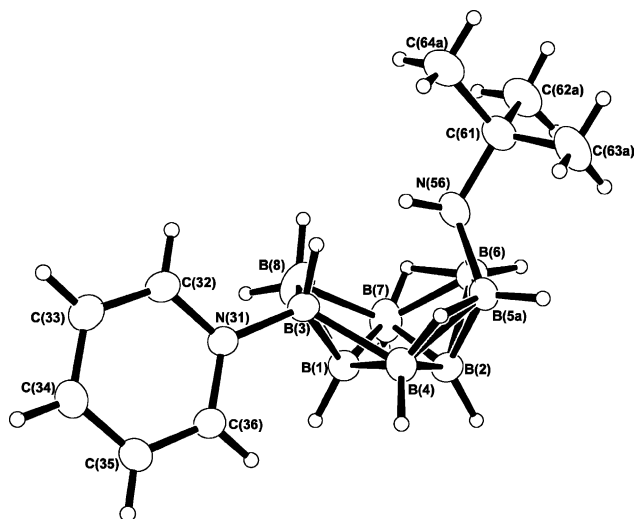


Fig. 5. A drawing of the crystallographically determined molecular structure of $[(C_5H_5N)B_8H_{11}NH^{ter}Bu]$ **20**, with thermal ellipsoids of non-hydrogen atoms shown at 50% probability. For clarity hydrogen atoms are drawn as circles with an arbitrary small radius. The crystal exhibits a 1:1 crystallographic disorder across a quasi-mirror-plane through N(5,6)B(6)B(1)B(3); one of the two similar derived molecules is drawn here. The two disordered molecules differ principally in the rotational orientations of the pyridine and tertiary-butyl moieties about the B(3)–N(31) and N(5,6)–C(61) linkages, respectively.

bulk samples. It is convenient to note here that the general NMR characteristics of this *hypho*-azanoborane compound type have been adequately covered in the previous literature [3–5]; all the new compounds reported in this present work exhibit typical behaviour.

Of the crystal structures, it should be noted that the {NH₂t} species **18** contained two independent molecules within the asymmetric unit of the unit cell, and therefore, two independent molecular structures are established for this compound. The {NH^{ter}Bu} compound **20**, by contrast, was subject to a 1:1 crystallographic disorder across a quasi-mirror-plane through N(5,6)B(6)B(1)B(3): although the molecular geometry for both forms was clearly established, including hydrogen-atom location, with clear parallels with the molecular structures of compounds **17**, **18** and **19**, any derived geometry may be insufficiently precise for detailed intercomparisons with these other species. The other two species, the {NHMe} and {NH^{iso}Pr} compounds, **17** and **19**, respectively, were crystallographically straightforward. The basic molecular structures of compounds **17**, **18**, **19** and **20** are found to be very similar, and similar in turn to those of the compounds in this class that have been previously examined structurally, viz. $[(EtNH_2)_8B_8H_{11}NH_2t]$, $[(^{iso}PrNH_2)_8B_8H_{11}NH^{iso}Pr]$, $[(^{iso}PrNH_2)_8B_8H_{11}NH^{ter}Bu]$ and $[(Et_2NH)_8B_8H_{11}NEt_2]$ [2,4,5]. There is of course variation among the substituent residues because that is how the compounds differ. There is, in principle, a systematic inductive/steric trend in the sequence {NHMe} →

{NH₂t} → {NH^{iso}Pr} → {NH^{ter}Bu}, but there is no corresponding large systematic variation in any molecular structural dimension, and, in any event, the {NH^{ter}Bu} species **20** is crystallographically not best defined, which inhibits a fine intercomparison across the whole of the series. The most significant variation, a relatively minor one, is in intra-cluster folding (Table 1).

Thus, there is a small, but interesting, and apparently systematic, change in the two intra-cluster fold-angles, as manifested by changes in the hinge-angle within the {B₈} cluster, and the hinge angle between the {B₈} cluster and the {B₂N} bridge triangle. Both these angles decrease somewhat along the **17** → **18** → **19** {NHMe} → {NH₂t} → {NH^{iso}Pr} sequence. This perhaps seems to go in the opposite direction from that naively expected from steric effects, which, it could be supposed instinctively, would force a more open fold-angle as the steric effect of the group increases. However, the groups are on the ‘outside’ of the cluster, and so perhaps that is why the opposite is observed. The effects are, however, small, so there may also be an electronic contribution to this effect. Alternatively, the observed variation could be a fortuitous consequence of solid-state packing effects, and not represent a systematic free-molecule effect. Here it is of interest to note that the trend does appear to be continued for the {NH^{ter}Bu} analogue **20**. However, since the crystal structure of this last species exhibited crystallographic disorder, and since the differences in these fold angles are small, there must be circumspection about the use of the derived dimensions of the molecular structure for such detailed comparison.

2.3. Molecular-orbital calculations

One aim of our theoretical research work is to explain the colour of pyridine–azanoborane complexes as part of a general theoretical understanding of this interesting and potentially important type of compound. One ultimate target here is to develop a qualitative molecular-orbital model to explain the UV–vis spectra of these azanoborane–pyridine derivatives in terms of a dependence on the substituents on the pyridine ring. For this purpose we have chosen ground-state calculation at the semi-empirical AM-1 level of theory [16]. This type of calculation gives the HOMO and LUMO energies, which we have used for interpretation. We did not use electronic spectra calculations that are only useful for directly comparing measured and calculated spectra, rather than energy-level differences, and which, therefore, do not allow any detailed view on how the substituents may influence the absorption maxima. At an initial empirical level, we were interested in an explanation for the dependence of the colour described by the longest wavelength absorption in terms of the nature of the substituents on the pyridine rings. In order to approach this, the AM-1 calculations were therefore,

Table 1

Selected intra-cluster fold-angles B(3)–B(4)–B(5), B(6)–B(7)–B(8), B(4)–B(5)–N(5,6) and B(7)–B(6)–N(5,6) (°) in [(C₅H₅N)B₈H₁₁NHMe] **17**, [(C₅H₅N)B₈H₁₁NH^{iso}Pr] **18**, [(C₅H₅N)B₈H₁₁NH^{ter}Bu] **20**

Compound		B(3)–B(4)–B(5)	B(6)–B(7)–B(8)	B(4)–B(5)–N(5,6)	B(7)–B(6)–N(5,6)
17	Me	116.7	117.65	118.9	119.4
18 (molecule 1)	Et	114.9	116.2	117.5	116.9
18 (molecule 2)	Et	114.8	115.7	117.4	116.0
19	^{iso} Pr	113.2	116.0	116.9	116.5
20	^{ter} Bu	107.0	114.5	116.4	109.1

Note that, for compound **20**, there is a 1:1 disorder of the molecule across the quasi-mirror-plane through N(5,6)B(6)B(1)B(3), which will render derived interatomic distances for this molecule unreliable for detailed comparisons.

carried out on the pyridine and substituted-pyridine species **17**, **22**, **24**, **25**, **26**, **27**, and **28**. Orbital energies after total geometry optimisation for the highest occupied molecular orbital (HOMO, see Fig. 6) and the lowest unoccupied molecular orbital (LUMO, again see Fig. 6) are listed in Table 2.

The orbital-energy differences $\Delta E_{\text{HOMO-LUMO}}$ show correlations with the experimental data for λ_{max} as determined from UV–vis absorption spectroscopy. Specifically, the plot of energy difference $\Delta E_{\text{HOMO-LUMO}}$ versus $1/\lambda_{\text{max}}$ is linear (Fig. 7). The only exception to this generality is [(4-NMe₂-C₅H₄N)B₈H₁₁NHMe] **22** which shows different behaviour: its datum is not coincident with the correlation line to which the data points for the other compounds are close. This exception perhaps arises because the dimethylaminopyridine ligand in compound **22** is a strong π -donor and thus not only affects the LUMO but also the HOMO. One tentative explanation is that the dimethylamino group acts as a concurrent π -donor towards the azanaborane unit.

The analysis of the results in Table 2 reveals that there is only a small variation in HOMO, and so the correlation in the $\Delta E_{\text{HOMO-LUMO}}$ plot arises principally from the larger variations in the LUMO. There is also a parallel with the LUMO energies of the individual uncomplexed pyridines. The starting aliphatic azanaboranes and the uncomplexed pyridines are both originally colourless, with λ_{max} for each smaller than 300 nm, and with the AM-1 calculated orbital-energy

differences being between 9 and 10 eV for the azanaboranes. Principal elements of the molecular-orbital structure that are responsible for the colour can be constructed qualitatively from combinations of fragments of HOMO of the azanaborane and the π -LUMO of the pyridine (Fig. 8).

The energy of the HOMO of the [(C₅H₅N)B₈H₁₁(NHR)] molecule is higher than that of the HOMO of the {B₈H₁₁(NHR)} fragment, and is nearly completely localised around the framework of the cluster (Fig. 6). Concomitantly, the LUMO of the molecule is localised exclusively on the pyridine fragment (Fig. 6) and is lower in energy than the LUMO of the pyridine fragment in pure pyridines (Fig. 8). The resulting calculated orbital-energy difference of between 6 and 7 eV is responsible for the absorption in the visible region. Due to the localisation of the LUMO of [(C₅H₅N)B₈H₁₁(NHR)] molecule on the complexed pyridine fragment, this orbital-energy difference and, therefore, also the colour show a dependence on the pyridine substituents. A π -donor leads to a blue shift whereas a π -acceptor leads to a red shift. The dimethylaminopyridine compound **22**, with the strongest donor substituent on the pyridine ring, and [(4-NO₂-C₅H₄N)B₈H₁₁NHMe] **27**, with the strongest acceptor substituent, define the limits of the observed wavelength range of 320–480 nm, within which all the other compounds reported here are found. This range, corresponding to 3.9–2.6 eV, represents the energy differences between ground and excited states of molecules,

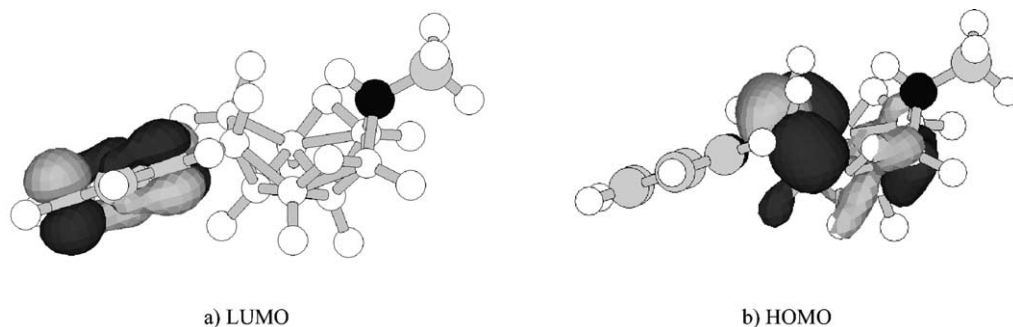


Fig. 6. AM1-calculated molecular orbitals of [(C₅H₅N)B₈H₁₁NHMe] **17**: (a) LUMO and (b) HOMO.

Table 2

Orbital energies after total geometry optimisation for the highest occupied molecular orbital (HOMO) and the lowest unoccupied molecular orbital (LUMO) for the substituted pyridine species [(RC₅H₄N)B₈H₁₁(NHR)]

AM1	UV-vis absorption $1/\lambda$ (cm ⁻¹)	HOMO (eV)	LUMO (eV)	ΔE (LUMO–HOMO) (eV)	LUMO (isolated pyridine derivatives) (eV)
Compound					
22	3.13	-7.70	-0.63	7.07	+0.51
17	2.75	-7.97	-1.05	6.92	+0.17
25	2.56	-8.07	-1.30	6.77	-0.32
24	2.41	-7.91	-1.29	6.62	-0.35
28	2.08	-7.92	-1.46	6.46	-0.55
26	2.60	-8.08	-1.69	6.39	-0.66
27	2.32	-8.34	-2.32	6.02	-1.39

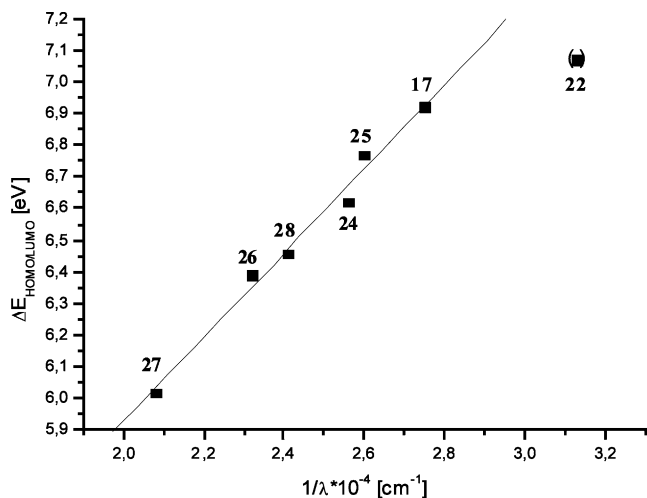


Fig. 7. Correlation of the energy differences $\Delta E_{\text{HOMO-LUMO}}$ with $1/\lambda_{\text{max}}$ for the series of pyridine and substituted pyridine compounds 17–28.

but is clearly much lower than the calculated HOMO–LUMO energy differences of between 6 and 7 eV. This is as expected from this type of calculation, because any Coulomb and exchange integrals and conformation interactions, especially of the excited state, are not considered, and these typically reduce the energy differences. Compared with the unsubstituted pyridine compound 17, the pyridine units of all the other compounds except the dimethylamino compound 22 are acceptor-substituted. Within this series of acceptor-substituted compounds, the LUMO energy can be reduced for a variety of reasons. Thus, in the brominated compound 25 there is found to be a strong inductive effect from the bromine substituent, in the 4-phenylpyridine compound 24 the phenyl moiety acts as a good π -acceptor, in the chinoline compound 28 the extended π -system can be invoked, whereas in the acetyl and nitro compounds 26 and 27 the involvement of the π^* orbitals of the carbonyl and nitro groups, respectively, are the principal factors in the reduction of the LUMO energy of the [(C₅H₅N)B₈H₁₁(NHR)] molecule compared with the pure pyridine. In contrast to the

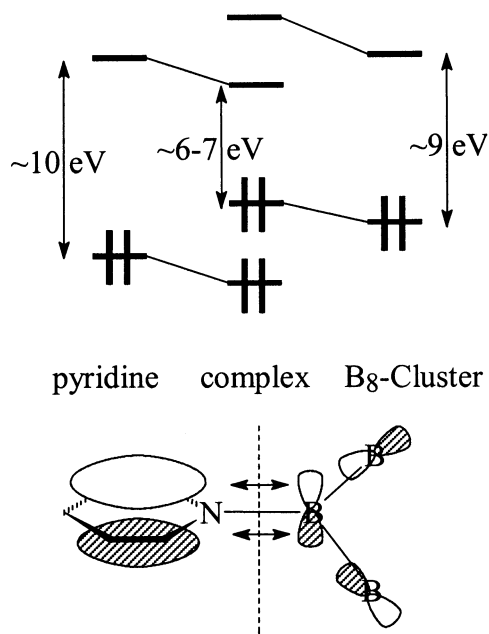


Fig. 8. Schematic picture of the energy difference $\Delta E_{\text{HOMO-LUMO}}$ in pure pyridine (left), in a [(C₅H₅N)B₈H₁₁(NHR)] molecule (centre) and in a [(RNH₂)B₈H₁₁(NHR)] molecule (right).

variations arising from changing the substituent on pyridine, changing the residue R of the aliphatic group on the bridging nitrogen atom does not show any significant effect on the λ_{max} value of the relevant {NHMe}, {NHEt}, {NH^{iso}Pr} and {NH^{ter}Bu} compounds 17, 18, 19 and 20. Calculations (which are not plotted in Fig. 6) reveal only a small variation among their HOMO energies, from 6.92 to 6.87 eV. This variation is too small to have any significant differential effects on the colours of these species.

It has been shown previously [11] that the colours of 6,9-bis-pyridine-*arachno*-decaborane [6,9-(C₅H₅N)₂-*arachno*-B₁₀H₁₂] and its ring-substituted derivatives vary from a very pale yellow to a deep red, depending on the substituent group on the pyridine ligand. In the case of [6,9-(C₅H₅N)₂-*arachno*-B₁₀H₁₂] and its ring-substituted derivatives, electron-withdrawing substituents also shifted the absorption band at the longest wave

length towards red, whereas a π -donor substituent led to a blue shift. The differences of cluster-structure character between ten-vertex *arachno* $\{B_{10}\}$ and eight-vertex *hypho* $\{B_8\}$ would, therefore, appear to have no significant differential influence on the colours of their pyridine complexes, because the $\{B_8\}$ series shows very similar colourations to the $\{B_{10}\}$ series [11]. In this regard it may be noted that for both systems the local structures at the point of pyridine attachment are very similar: in each case the pyridine ligand is bound to a cluster $\{BH(endo)\}$ unit. It will clearly be of interest to examine other pyridine–boranes in this respect: for example, those involving the ligand *endo*-bound to an open face $\{BH(exo)\}$ unit, or *exo* to an open face boron atom that is not associated with an inner-sphere bridging or *endo* hydrogen atom, or bound *exo* to an apical boron atom.

Due to the absence of crystallographic X-ray data for the substituted pyridine derivatives **21**–**27**, it has not been possible to compare their calculated and experimental geometries, especially for the conformation about the B–N(pyridine) bond, which is the most flexible point in the structure. Nevertheless, because the results of our calculations suggest a strong dependence of the absorption maxima in UV–vis spectra on the LUMO energy of the substituted pyridines, it seems likely that changes in the rotamer conformation about the B–N(pyridine) vector should not have a strong influence on the LUMO of the pyridine moiety and therefore on the absorption maxima. Further calculations, especially of the dependence of the rotational barrier about the B–N(pyridine) vector, are needed to test this hypothesis. Interesting in this regard would be additional information about the different behaviour of derivative **22**, which contains a strong π -donor substituent and therefore, could act as a π -donor into the $\{B_8\}$ cluster.

3. Experimental

Reactions were carried out in dry solvents. The starting azanonaboranes $[(RNH_2)B_8H_{11}NHR]$, where R is methyl **1**, ethyl **2**, *isopropyl* **3**, and tertiary butyl **4**, were prepared according to the literature [1,4,5], and $[B_9H_{13}(SMe_2)]$ was also prepared by a literature method [1]. Preparative thin-layer chromatography was carried out using 0.75 mm layers of silica-gel G (Merck GF₂₅₄) made from water slurries on glass plates of dimensions of 20×20 cm², followed by drying in air at 100 °C. All other reagents were obtained commercially. NMR spectroscopy was carried out at 4.7 T on commercially available instrumentation. Chemical shifts δ are given in ppm to high field (low frequency) of TMS for ¹H (Ξ nominally 100 MHz) and ¹³C (Ξ nominally 25.145004 MHz), and $[BF_3(OEt)]$ for ¹¹B (Ξ nominally 32.083971

MHz) [14], Ξ being as defined by McFarlane [15]. Mass spectrometric data were measured using a Finnigan MAT 8222 instrument, either (a) by fast-atom bombardment ionisation (FAB) with glycerol or nitrobenzylalcohol (NBA) as matrix, or (b) by 70 eV electron-impact ionisation (EI) at 473 K. Only the signal with the highest intensity of the boron isotopic pattern is listed. UV data were measured on a Varian Cary 50 Bio instrument. Molecular-orbital calculations [16] were carried out with HYPERCHEM [17].

3.1. X-ray diffraction analysis

Crystal data for $[(C_5H_5N)B_8H_{11}NHMe]$ **17**, $[(C_5H_5N)B_8H_{11}NHET]$ **18**, $[(C_5H_5N)B_8H_{11}NH^{iso}Pr]$ **19** and $[(C_5H_5N)B_8H_{11}NH^{ter}Bu]$ **20** are as follows: compound **17**, $C_6H_{20}B_8N_2$: $M = 206.72$, triclinic (from dichloromethane), $0.34 \times 0.31 \times 0.11$ mm, Space group $P\bar{1}$, $a = 6.6798(4)$, $b = 9.4555(4)$, $c = 11.4955(7)$ Å, $\alpha = 111.494(3)$, $\beta = 89.971(3)$, $\gamma = 106.3404(3)^\circ$, $U = 644.13(6)$ Å³, $D_{calc} = 1.066$ Mg m⁻³, $Z = 2$, Mo–K α , $\lambda = 0.71073$ Å, $\mu = 0.054$ mm⁻¹, $T = 150(2)$ K, $R_1 = 0.0455$ for 2269 reflections with $I > 2\sigma(I)$, and $wR_2 = 0.1194$ for all 2491 independent reflections; compound **18**, $C_7H_{22}B_8N_2$: $M = 220.75$, triclinic (from dichloromethane), $0.40 \times 0.08 \times 0.02$ mm, Space group $P\bar{1}$, $a = 10.2693(2)$, $b = 11.9478(3)$, $c = 12.12373(3)$ Å, $\alpha = 81.7440(11)$, $\beta = 76.85960(10)$, $\gamma = 87.3380(10)^\circ$, $U = 1431.87(6)$ Å³, $D_{calc} = 1.024$ Mg m⁻³, $Z = 4$, Mo–K α , $\lambda = 0.71073$ Å, $\mu = 0.052$ mm⁻¹, $T = 150(2)$ K, $R_1 = 0.0683$ for 3641 reflections with $I > 2\sigma(I)$, and $wR_2 = 0.1820$ for all 5612 independent reflections; compound **19**, $C_8H_{24}B_8N_2$: $M = 234.77$, triclinic (from dichloromethane), $0.48 \times 0.42 \times 0.10$ mm, Space group $P\bar{1}$, $a = 7.1388(5)$, $b = 9.1147(9)$, $c = 12.7128(13)$ Å, $\alpha = 102.804(4)$, $\beta = 103.586(5)$, $\gamma = 103.573(5)^\circ$, $U = 747.32(12)$ Å³, $D_{calc} = 1.043$ Mg m⁻³, $Z = 2$, Mo–K α , $\lambda = 0.71073$ Å, $\mu = 0.053$ mm⁻¹, $T = 150(2)$ K, $R_1 = 0.0574$ for 2229 reflections with $I > 2\sigma(I)$, and $wR_2 = 0.1683$ for all 2926 independent reflections; compound **20**, $C_9H_{26}B_8N_2$: $M = 248.79$, monoclinic (from dichloromethane), Space group $P2_1/n$, $a = 6.9056(1)$, $b = 32.4995(4)$, $c = 7.4161(1)$ Å, $\beta = 99.6579(6)^\circ$, $U = 1640.79(3)$ Å³, $D_{calc} = 1.007$ Mg m⁻³, $Z = 4$, Mo–K α , $\lambda = 0.71073$ Å, $\mu = 0.052$ mm⁻¹, $T = 150(2)$ K, $R_1 = 0.0514$ for 2568 reflections with $I > 2\sigma(I)$, and $wR_2 = 0.1271$ for all 3205 independent reflections. CCDC reference numbers for compounds **17**, **18**, **19** and **20** are 172 012, 172 013, 172 014 and 172 015, respectively. Methods and programs were standard [18].

3.2. Preparation of compounds

3.2.1. General procedure

The appropriate compound $[(RNH_2)B_8H_{11}NHR]$, where R = methyl **1**, ethyl **2**, *isopropyl* **3**, or *tert*-butyl

4 (100 μmol) was dissolved in 10 ml benzene, and the appropriate amine or pyridine for the ligand-exchange reaction was added (100 μmol). After heating the solution at reflux for 2 h, the solvent was removed under reduced pressure. The residue, consisting of the crude azanonaborane product, was then purified by repeated thin-layer chromatography on silica gel using dichloromethane as liquid phase. Criteria of purity and identity for this well-recognised molecular type [1–5] were clean multinuclear NMR spectra consistent with the molecular formulation, allied with corresponding molecular ions in the mass spectrum, and also allied, in the case of compounds **17**, **18**, **19** and **20** as representatives, with all-atom molecular structures determined by single crystal X-ray diffraction analysis as summarised above.

3.2.2. Primary amines

3.2.2.1. [*(EtNH₂)B₈H₁₁NHMe*] **5**. Compound **1** reacts with ethylamine to give **5**. $R_F = 0.80$. Yield: 35% (6 mg; 35 μmol); NMR (CDCl_3): BH(2) -55.2 [-0.77], BH(7) -33.3 [$+0.50$], BH(4) -33.1 [$+0.50$], BH₂(8) -30.9 [*endo* -0.77 , *exo* $+0.50$], BH(3) -20.5 [$+0.91$], BH(5) and BH(6) both at ca. -10.3 [both at ca. $+2.23$], BH(1) $+1.4$ [$+2.39$]; $\mu\text{H}(4.5) = -2.15$, $\mu\text{H}(6.7) = -2.32$; NH₂CH₂CH₃ $+44.9$ [$+2.84$], NHCH₃ $+38.7$ [$+2.23$], NH₂CH₂CH₃ $+13.9$ [$+1.71$], NH₂CH₂CH₃ [$+5.17$] and NHCH₃ [-1.28]. Mass spectrum: FAB (NBA) m/z 172 ($[\text{M}]^+$, 20%), m/z 172 ($[\text{M}]^-$, 17%).

3.2.2.2. [*(^{iso}PrNH₂)B₈H₁₁NHMe*] **6**. Compound **1** reacts with *isopropylamine* to give **6**. $R_F = 0.76$; Yield: 38% (7 mg, 38 μmol); NMR (CDCl_3): BH(2) -55.1 [-0.62]; BH(7) -34.2 [$+0.76$]; BH(4) -32.8 [$+0.76$]; -30.9 [*endo* -0.62 , *exo* $+0.52$] BH₂(8); BH(3) -20.9 [$+1.23$]; BH(5) and BH(6) both at ca. -10.2 [both at ca. $+2.42$]; BH(1) $+1.4$ [$+2.58$]; $\mu\text{H}(4.5) = -1.95$; $\mu\text{H}(6.7) = -2.09$; NH₂CH(CH₃)₂ $+50.3$ [$+3.48$]; NHCH₃ $+37.6$ [$+2.40$]; NH₂CH(CH₃)₂ $+20.7/+20.4$ [$+1.40$]; NH₂CH(CH₃)₂ [$+3.98$] and NHCH₃ [-1.34]; Mass spectrum: FAB (NBA): m/z : 186 ($[\text{M}]^+$, 65%), m/z : 186 ($[\text{M}]^-$, 18%).

3.2.2.3. [*(^{ter}BuNH₂)B₈H₁₁NHMe*] **7**. Compound **1** reacts with *tert*-butylamine to give **7**. $R_F = 0.89$; Yield: 34% (7 mg, 34 μmol); NMR (CDCl_3): BH(2) -55.2 [-0.83]; BH(7) -34.6 [$+0.37$]; BH(4) -32.1 [$+0.37$]; BH₂(8) -30.1 [*endo* -0.83 , *exo* $+0.27$]; BH(3) -23.2 [$+0.84$]; BH(5) and BH(6) both at ca. -10.4 [both at ca. $+2.07$]; BH(1) $+0.6$ [$+2.26$]; $\mu\text{H}(4.5)/\mu\text{H}(6.7) = -2.30$; NH₂C(CH₃)₃ $+53.9$; NHCH₃ $+37.6$ [$+2.12$]; NH₂C(CH₃)₃ $+27.2$ [$+1.17$]; NH₂C(CH₃)₃ [$+4.96/+4.80$]; NHCH₃ [-1.38]; Mass spectrum: FAB (NBA): m/z : 200 ($[\text{M}]^+$, 100%); 352 ($[\text{M}+\text{NBA}-2\text{H}]^+$, 6%), m/z : 200 ($[\text{M}]^-$, 40%).

3.2.2.4. [*{MeO(CH₂)₃NH₂}B₈H₁₁NHMe*] **8**. Compound **1** reacts with 3-methoxypropylamine to give **8**. Chromatography: CH₂Cl₂/THF (9:1); $R_F = 0.77$; Yield: 42% (9 mg, 42 μmol); NMR (CDCl_3): BH(2) -55.1 [-0.68]; BH(7) -33.6 [$+0.70$]; BH(4) -32.3 [$+0.70$]; BH₂(8) -32.3 [*endo* -0.68 , *exo* $+0.48$]; BH(3) -20.5 [$+1.13$]; BH(5) and BH(6) both at ca. -9.8 [both at ca. $+2.38$]; BH(1) $+1.9$ [$+2.56$]; $\mu\text{H}(4.5) = -1.97$; $\mu\text{H}(6.7) = -2.09$; CH₂OCH₃ $+73.1$ [$+3.62$]; OCH₃ $+59.2$ [$+3.37$]; NH₂CH₂ $+50.5$ [$+3.24$]; NH₂CH₂CH₂ $+27.6$ [$+1.93$]; NHCH₃ $+38.4$ [$+2.38$]; NH₂(CH₂)₃OCH₃ [$+4.77$]; NHCH₃ [-1.32]; Mass spectrum: FAB (NBA): m/z : 216 ($[\text{M}]^+$, 10%), m/z : 216 ($[\text{M}]^-$, 35%); 201 [$[\text{M}-\text{CH}_3]^-$, 40%).

3.2.2.5. [*{HO(CH₂)₃NH₂}B₈H₁₁NHMe*] **9**. Compound **1** reacts with 3-hydroxypropylamine to give **9**. Chromatography: CH₂Cl₂/THF (9:1); $R_F = 0.27$; Yield: 31% (6 mg, 31 μmol); NMR (CDCl_3): BH(2) -55.2 [-0.71]; BH(7) -32.4 [$+0.67$]; BH(4) -32.4 [$+0.67$]; BH₂(8) -32.4 [*endo* -0.71 , *exo* $+0.43$]; BH(3); -20.4 [$+1.11$]; BH(5) and BH(6) both at ca. -9.7 [both at ca. $+2.37$]; BH(1) $+1.7$ [$+2.49$]; $\mu\text{H}(4.5) = -2.00$; $\mu\text{H}(6.7) = -2.11$; CH₂OH $+63.0$ [$+3.90$]; NH₂CH₂ $+50.1$ [$+3.24$]; NHCH₃ $+38.5$ [$+2.38$]; CH₂CH₂OH $+29.0$ [$+1.94$]; NH₂(CH₂)₃OH [$+4.95/+4.83$]; NHCH₃ [-1.31]; Mass spectrum: FAB (NBA): m/z : 202 ($[\text{M}]^+$, 45%), m/z : 202 ($[\text{M}]^-$, 52%); 188 [$[\text{M}-\text{CH}_3+\text{H}]^-$, 43%).

3.2.2.6. [*{OC₄H₈NH(CH₂)₂NH₂}B₈H₁₁NHMe*] **10**. Compound **1** reacts with 4-(2-aminoethyl)morpholine to give **10**. Chromatography: CH₂Cl₂/THF (3:1); $R_F = 0.66$; Yield: 22% (7 mg, 22 μmol); NMR (CDCl_3): BH(2) -55.2 [-0.69]; BH(4) and BH(7) -32.5 [$+0.70$]; BH₂(8) -32.5 [*endo* -0.69 , *exo* $+0.47$]; BH(3) -20.3 [$+1.15$]; BH(5) and BH(6) both at ca. -9.9 [both at ca. $+2.35$]; BH(1) $+1.7$ [$+2.53$]; $\mu\text{H}(4.5) = -1.99$; $\mu\text{H}(6.7) = -2.10$; NCH₂CH₂O $+66.8$ [$+3.76$]; NH₂CH₂CH₂N $+54.9$ [$+2.59$]; NCH₂ $+53.0$ [$+2.73$]; NH₂CH₂CH₂N $+45.7$ [$+3.16$]; NHCH₃ $+38.4$ [$+2.41$]; NH₂CH₂CH₂N [$+4.85$]; NHCH₃ [-1.33]; Mass spectrum: FAB (NBA): m/z : 257 ($[\text{M}]^+$, 25%), m/z : 257 ($[\text{M}]^-$, 38%).

3.2.3. Secondary amines

3.2.3.1. [*(C₄H₈NH)B₈H₁₁NHMe*] **11**. Compound **1** reacts with pyrrolidine to give **11**. $R_F = 0.89$; Recrystallisation EtOH/H₂O 1:1; Yield: 45% (9 mg, 45 μmol); NMR (CDCl_3): BH(2) -55.0 [-0.68]; BH(4) and BH(7) -33.0 [$+0.73$]; BH₂(8) -33.0 [*endo* -0.68 , *exo* $+0.53$]; BH(3) -16.7 [$+1.16$]; BH(5) and BH(6) both at ca. -9.9 [both at ca. $+2.59$]; BH(1) $+1.5$ [$+2.43$]; $\mu\text{H}(4.5) = -1.95$; $\mu\text{H}(6.7) = -2.13$; NHCH₂ $+56.9/+56.4$ [$+3.57/+3.11$]; NHCH₃ $+34.4$ [$+2.39$]; NHCH₂CH₂ $+24.4/+24.2$ [$+2.07$]; NHCH₂ [$+4.24$];

NH [−1.33]; Mass spectrum: FAB (NBA): m/z : 198 ($[M]^+$, 40%), m/z : 198 ($[M]^-$, 30%).

3.2.3.2. $[(C_4H_8NH)B_8H_{11}NH^{iso}Pr]$ **12**. Compound **3** reacts with pyrrolidine to give **12**. $R_F = 0.88$; Recrystallisation EtOH/H₂O 1:1; Yield: 42% (10 mg, 42 μ mol); NMR (CDCl₃): BH(2) −55.5 [−0.68]; BH(4) and BH(7) −32.7 [+0.76]; BH₂(8) −32.7 [*endo* −0.68, *exo* +0.53]; BH(3) −16.9 [+1.21]; BH(5) and BH(6) both at ca. −11.2 [both at ca. +2.59]; BH(1) +1.4 [+2.43]; μ H(4.5) = −2.02; μ H(6.7) = −2.21; NHCH₂ +56.9/+56.5 [+3.58/+3.12]; NHCH +52.7 [+2.53]; NHCH₂CH₂ +24.4/+24.3 [+2.07]; NHCH(CH₃)₂ +21.3/+21.2 [+1.06]; NHCH₂ [+4.20]; NH [−1.65]; Mass spectrum: FAB (NBA): m/z : 226 ($[M]^+$, 100%), m/z : 226 ($[M]^-$, 38%).

3.2.3.3. $[(C_5H_{10}NH)B_8H_{11}NHMe]$ **13**. Compound **1** reacts with piperidine to give **13**. Chromatography: CH₂Cl₂/THF (10:1); $R_F = 0.86$; Yield: 50% (11 mg, 50 μ mol); NMR (CDCl₃): BH(2) −55.2 [−0.74]; BH(7) −33.6 [+0.70]; BH(4) −33.4 [+0.70]; BH₂(8) −32.0 [*endo* −0.74, *exo* +0.58]; BH(3) −16.1 [+1.11]; BH(5) and BH(6) both at ca. −10.1 [both at ca. +2.45]; BH(1) +1.3 [+2.60]; μ H(4.5) = −1.96; μ H(6.7) = −2.16; NHCH₂CH₂ +55.5/+55.2 [+3.76/+2.80]; NHCH₂CH₂/NHCH₂CH₂CH₂ +25.3/+22.2 [+2.10 bis +1.40]; NHCH₃ +38.4 [+2.41]; NHCH₂CH₂CH₂CH₂ [+3.19]; NHCH₃ [−1.34]; Mass spectrum: FAB (NBA): m/z : 212 ($[M]^+$, 60%), m/z : 212 ($[M]^-$, 18%).

3.2.3.4. $[(NHC_4H_8NH)B_8H_{11}NHMe]$ **14**. Compound **1** reacts with piperazine to give **14**. Chromatography: CH₂Cl₂/THF (1:1); $R_F = 0.84$; Yield: 46% (10 mg, 46 μ mol); NMR (*d*₈-THF): BH(2) −57.2 [−0.63]; BH(4) and BH(7) −36.1 [+0.58]; BH₂(8) −32.9 [*endo* −0.63, *exo* +0.58]; BH(3) −17.9 [+1.00]; BH(5) and BH(6) both at ca. −12.2 [both at ca. +2.26]; BH(1) +1.0 [+2.51]; μ H(4.5) = −2.14; μ H(6.7) = −2.29; Cluster-NHCH₂ +55.5/+55.3 [+3.41/2.8]; Cluster-NHCH₂CH₂ +44.7/44.6 [+2.8−3.0]; NHCH₃ +38.4 [+2.28]; Cluster-NHCH₂ [+5.19]; Cluster-NHCH₂CH₂NH [+2.50]; NH [−0.79]; Mass spectrum: FAB (NBA): m/z : 213 ($[M]^+$, 35%), m/z : 213 ($[M]^-$, 8%).

3.2.3.5. $[(OC_4H_8NH)B_8H_{11}NHMe]$ **15**. Compound **1** reacts with morpholine to give **15**. Chromatography: CH₂Cl₂/THF (15:1); $R_F = 0.79$; Yield: 28% (6 mg, 28 μ mol); NMR (CDCl₃): BH(2) −54.9 [−0.90]; BH(4) and BH(7) −33.4 [+0.35]; BH₂(8) −31.4 [*endo* −0.90, *exo* +0.35]; BH(3) −15.9 [+0.81]; BH(5) and BH(6) both at ca. −9.9 [both at ca. +2.15/+2.09]; BH(1) +1.2 [+2.37]; μ H(4.5) = −2.24; μ H(6.7) = −2.44; NHCH₂CH₂O +64.3/+64.1 [+3.75/+3.70]; NHCH₂ +53.3/+53.1 [+3.16/+2.77]; NHCH₃ +37.8 [+2.12];

NHCH₂CH₂O [+5.25]; NHCH₃ [−1.38]; Mass spectrum: FAB (NBA): m/z : 214 ($[M]^+$, 28%), m/z : 214 ($[M]^-$, 5%).

3.2.3.6. $[\{CHNH(CH)_2N\}B_8H_{11}NHMe]$ **16**. Compound **1** reacts with imidazol to give **16**. Chromatography: CH₂Cl₂/THF (1:1); $R_F = 0.78$; Yield: 38% (7 mg, 38 μ mol); NMR (*d*₈-THF): BH(2) −55.1 [−0.73]; BH₂(8) −34.2 [*endo* −0.52, *exo* +0.50]; BH(4) and BH(7) −31.3 [+0.59]; BH(3) −20.8 [+1.70]; BH(5) and BH(6) both at ca. −10.7 [both at ca. +2.24]; BH(1) +0.5 [+2.69]; μ H(4.5)/ μ H(6.7) = −1.99; NCHNH +136.1 [+8.05]; NHCH +127.2 [+7.22]; NCH +117.6 [+6.91]; NHCH₃ +38.9 [+2.24]; NH_{bridge} [−1.06]; NH [+12.3]; Mass spectrum: FAB (NBA): m/z : 195 ($[M]^+$, 15%), m/z : 195 ($[M]^-$, 30%).

3.2.4. Pyridine and pyridine derivatives

3.2.4.1. $[(C_5H_5N)B_8H_{11}NHMe]$ **17**. Compound **1** reacts with pyridine to give **17**. $R_F = 0.64$; Yield: 40% (8 mg, 40 μ mol); NMR (CDCl₃): BH(2) −54.6 [−0.49]; BH(7) −32.4 [+0.93]; BH(4) −29.3 [+0.93]; BH₂(8) −29.3 [*endo* −0.25, *exo* +0.77]; BH(3) −15.5 [+2.13]; BH(5) and BH(6) both at ca. −10.5 and −9.2 [both at ca. +2.51/+2.43]; BH(1) +1.9 [+2.94]; μ H(4.5)/ μ H(6.7) = −1.69; NCHCHCH +147.5 [+8.97]; NCHCHCH +140.3 [+7.99]; NCHCHCH +125.2 [+7.54]; NHCH₃ +38.5 [+2.48]; NH [−1.06]; Mass spectrum: FAB (NBA, cosolvens: CH₂Cl₂): m/z : 206 ($[M]^+$, 89%); UV spectrum: $\lambda_{max} = 364$ nm (THF; 2.7×10^{-4} mol l^{−1}; $\epsilon = 2259$).

3.2.4.2. $[(C_5H_5N)B_8H_{11}NHEt]$ **18**. Compound **2** reacts with pyridine to give **18**. $R_F = 0.74$; Yield: 59% (13 mg, 59 μ mol); NMR (CDCl₃): BH(2) −54.7 [−0.52]; BH(7) −32.3 [+0.92]; BH(4) −29.2 [+0.92]; BH₂(8) −29.2 [*endo* −0.24, *exo* +0.77]; BH(3) −15.4 [+2.43]; BH(5) and BH(6) both at ca. −11.2 [both at ca. +2.51/+2.43]; BH(1) +2.0 [+2.94]; μ H(4.5)/ μ H(6.7) = −1.72; NCHCHCH +147.5 [+8.94]; NCHCHCH +140.4 [+8.00]; NCHCHCH +125.2 [+7.54]; NHCH₂ +46.5 [+2.69]; NHCH₂CH₃ +13.6 [+1.11]; NH [−1.15]; Mass spectrum: FAB (NBA): m/z : 220 ($[M]^+$, 44%); EI (70 eV, 473 K): m/z : 220 ($[M]^+$, 20%), 217 ($[M-3H]^+$, 30%); UV spectrum: $\lambda_{max} = 364$ nm (THF; 2.9×10^{-4} mol l^{−1}; $\epsilon = 2034$).

3.2.4.3. $[(C_5H_5N)B_8H_{11}NH^{iso}Pr]$ **19**. Compound **3** reacts with pyridine to give **19**. $R_F = 0.67$; Yield: 47% (11 mg, 47 μ mol); NMR (CDCl₃): BH(2) −55.0 [−0.57]; BH(7) −32.2 [+0.92]; BH(4) −29.3 [+0.97]; BH₂(8) −29.3 [*endo* −0.25, *exo* 0.76]; BH(3) −15.8 [+2.11]; BH(5) and BH(6) both at ca. −11.8/−10.2 [both at ca. +2.55/45]; BH(1) +1.8 [+2.96]; μ H(4.5)/ μ H(6.7) = −1.76; NCHCHCH +147.6 [+8.98];

NCHCHCH +140.5 [+7.99]; NCHCHCH +125.2 [+7.53]; NHCH +52.9 [+2.53]; NHCH(CH₃)₂ +21.3/+21.2 [+1.11]; NH [-1.36]; Mass spectrum: FAB (NBA): *m/z*: 234 ([M]⁺, 20%); UV spectrum: λ_{max} = 364 nm (THF; 3.2 × 10⁻⁴ mol l⁻¹; ε = 1968).

3.2.4.4. [(C₅H₅N)B₈H₁₁NH^{ter}Bu] **20**. Compound **4** reacts with pyridine to give **20**. R_F = 0.69; Yield: 53% (13 mg, 53 μmol); NMR (d₈-THF): BH(2) -55.2 [-0.56]; -31.9 [*endo* -0.19, *exo* +0.79] BH₂(8); BH(4) and BH(7) -29.1 [+0.98]; BH(3) -15.4 [+2.18]; BH(5) and BH(6) both at ca. -11.3 [both at ca. +2.66/+2.58]; BH(1) +2.4 [+2.98]; μH(4.5)/μH(6.7) = -1.93; NCHCHCH +147.6 [+8.99]; NCHCHCH +140.2 [+8.01]; NCHCHCH +125.2 [+7.55]; NHC(CH₃)₃ +53.3; NHC(CH₃)₃ +27.3 [+1.12]; NH [-1.12]; Mass spectrum: FAB (NBA): *m/z*: 248 ([M]⁺, 100%), *m/z*: 249 ([M]⁻, 20%); UV spectrum: λ_{max} = 364 nm (THF; 2.6 × 10⁻⁴ mol l⁻¹; ε = 2307).

3.2.4.5. [(4-NH₂C₅H₄N)B₈H₁₁NHMe] **21**. Compound **1** reacts with 4-aminopyridine to give **21**. Chromatography: CH₂Cl₂/THF (3:1); R_F = 0.68; Yield: 47% (10 mg, 47 μmol); NMR (THF): BH(2) -56.8 [-0.68]; BH(7) -35.8 [+0.63]; BH(4) -33.1 [+0.63]; BH₂(8) -32.9 [*endo* -0.35, *exo* +0.63]; BH(3) -17.6 [+1.85]; BH(5) and BH(6) both at ca. -12.3 [both at ca. +2.31]; BH(1) +0.6 [+2.71]; μH(4.5)/μH(6.7) = -1.96; CNH₂ +158.2; NCHCHC +150.7 [+8.23]; NCHCHC +109.8 [+6.51]; NHCH₃ +39.1 [+2.31]; NH [-0.70]; NH₂ [+6.61]; Mass spectrum: FAB: *m/z* (Glycerin, cosolvent THF): 221 ([M]⁺, 10%), *m/z* (NBA): 221 ([M]⁻, 5%).

3.2.4.6. [(4-NMe₂-C₅H₄N)B₈H₁₁NHMe] **22**. Compound **1** reacts with 4-dimethylaminopyridine to give **22**. R_F = 0.67; Yield: 57% (14 mg, 57 μmol); NMR (THF): BH(2) -54.7 [-0.58]; BH₂(8) -33.6 [*endo* -0.42, *exo* +0.65]; BH(4) and BH(7) -30.6 [+0.79]; BH(3) -15.8 [+1.94]; BH(5) and BH(6) both at ca. -10.1 [both at ca. +2.42]; BH(1) +0.9 [+2.84]; μH(4.5)/μH(6.7) = -1.79; CN(CH₃)₂ +155.1; NCHCHC +146.2 [+8.34]; NHCHCHC +106.1 [+6.51]; N(CH₃)₂ +39.6 [+3.13]; NHCH₃ +38.3 [+2.42]; NH [-1.14]; Mass spectrum: FAB (NBA): *m/z*: 249 ([M]⁺, 18%); UV spectrum: λ_{max} = 320 nm (THF; 7.5 × 10⁻⁵ mol l⁻¹; ε = 8400).

3.2.4.7. [(4-PhCH₂-C₅H₄N)B₈H₁₁NHMe] **23**. Compound **1** reacts with 4-benzylpyridine to give **23**. R_F = 0.67; Yield: 55% (16 mg, 55 μmol); NMR (THF): BH(2) -54.6 [-0.51]; BH₂(8) -32.6 [*endo* -0.26, *exo* +0.73]; BH(4) and BH(7) -29.6 [+0.89]; BH(3) -15.5 [+2.06]; BH(5) and BH(6) both at ca. -10.4 [both at ca. +2.46]; BH(1) +1.8 [+2.93]; μH(4.5)/μH(6.7) = -1.69; C_{pyridin} +156.0; NCHCHC +146.9 [+8.76]; C_{benzyl} +136.6; C₆H₄ +129.1/127.3 [7.45–7.18]; NCHCHC +125.3 [+

7.25–7.45]; NHCH₃ [-1.30]; CH₂ +41.1 [+4.09]; NHCH₃ +38.5 [+2.46]; NH [-1.06]; Mass spectrum: FAB (NBA): *m/z*: 296 ([M]⁺, 45%), *m/z*: 296 ([M]⁻, 10%); UV spectrum: λ_{max} = 363 nm (THF; 1.0 × 10⁻⁴ mol l⁻¹; ε = 6100).

3.2.4.8. [(4-Ph-C₅H₄N)B₈H₁₁NHMe] **24**. Compound **1** reacts with 4-phenylpyridine to give **24**. R_F = 0.65. Yield: 50% (14 mg, 50 μmol); NMR (THF): BH(2) -55.0 [-0.76]; BH₂(8) -32.9 [*endo* -0.50, *exo* +0.51]; BH(4) and BH(7) -29.8 [+0.66]; BH(3) -16.1 [+1.83]; BH(5) and BH(6) both at ca. -10.6 [both at ca. +2.18]; BH(1) +2.6 [+2.72]; μH(4.5)/μH(6.7) = -1.94; C_{pyridin} +152.5; +147.7 [+8.63] (NCHCHC); C_{phenyl} +135.1; CCHCHCH +131.0 [+7.25–7.45]; CCHCHCH +129.6 [+7.25–7.45]; CCHCHCH +127.2 [+7.25–7.45]; NCHCHC +122.6 [+7.25–7.45]; NHCH₃ [-1.30]; Mass spectrum: FAB (NBA): *m/z*: 282 ([M]⁺, 35%), *m/z*: 283 ([M]⁻, 8%); UV spectrum: λ_{max} = 391 nm (THF; 6.6 × 10⁻⁵ mol l⁻¹; ε = 5000).

3.2.4.9. [(3-Br-C₅H₄N)B₈H₁₁NH^{iso}Pr] **25**. Compound **3** reacts with 3-bromopyridine to give **25**. R_F = 0.71; Yield: 45% (14 mg, 45 μmol); NMR (THF): BH(2) -54.9 [-0.51]; BH₂(8) -31.7 [*endo* -0.17, *exo* +0.77]; BH(4) and BH(7) -28.7 [+0.99]; BH(3) -15.7 [+2.09]; BH(5) and BH(6) both at ca. -11.6 [both at ca. +2.46]; BH(1) +2.0 [+2.97]; μH(4.5)/μH(6.7) = -1.75; NCHC +149.2 [+9.10]; NCHCHCH +146.5 [+8.10]; NCHCHCH +143.5 [+8.95]; NCHCHCH +126.4 [+7.39]; NHCH(CH₃)₂ +52.9 [+2.63]; NHCH(CH₃)₂ +21.3/+21.2 [+1.12]; NH [-1.06]; Mass spectrum: FAB (NBA): *m/z*: 312 ([M]⁺, 35%); UV spectrum: λ_{max} = 385 nm (THF; 7.5 × 10⁻⁵ mol l⁻¹; ε = 5333).

3.2.4.10. [(4-MeCO-C₅H₄N)B₈H₁₁NHMe] **26**. Compound **1** reacts with 4-acetylpyridine to give **26**. R_F = 0.6; Yield: 36% (9 mg, 36 μmol); NMR (CDCl₃): BH(2) -54.4 [-0.48]; BH₂(8) -31.7 [*endo* -0.13, *exo* +0.80]; BH(4) and BH(7) -28.6 [+0.97]; BH(3) -15.7 [+2.09]; BH(5) and BH(6) both at ca. -10.4 [both at ca. +2.48]; BH(1) +2.1 [+3.02]; μH(4.5)/μH(6.7) = -1.64; CO +194.2; NCHCHC +148.2 [+9.10]; NCHCHC +123.2 [+7.93]; NHCHCHC +144.9; COCH₃ +26.8 [+2.70]; NHCH₃ +38.6 [+2.50]; NH [-0.98]; Mass spectrum: FAB (NBA): *m/z*: 248 ([M]⁺, 45%), *m/z*: 248 ([M]⁻, 15%); UV spectrum: λ_{max} = 431 nm (THF; 2.2 × 10⁻⁴ mol l⁻¹; ε = 4000).

3.2.4.11. [(4-NO₂-C₅H₄N)B₈H₁₁NHMe] **27**. Compound **1** reacts with 4-nitropyridine to give **27**. R_F = 0.81; Yield: 16% (4 mg, 16 μmol); NMR (CDCl₃): BH(2) -54.7 [-0.50]; BH₂(8) -30.6 [*endo* +0.09, *exo* +0.85]; BH(4) and BH(7) -27.5 [+0.90]; BH(3) -15.4 [+2.13]; BH(5) and BH(6) both at ca. -10.2 [both at ca. +2.47]; BH(1) +2.4 [+3.00]; μH(4.5)/μH(6.7) = -1.66;

NCHCHC +150.7 [+9.27]; **NCHCHC** +119.4 [+8.23]; **NHCHCHC** +148.1; **NCH₃** +38.5 [+2.46]; **NH** [-0.98]; Mass spectrum: FAB (NBA): *m/z*: 251 ([M]⁺, 41%); UV spectrum: λ_{max} = 480 nm (THF; 6.8 × 10⁻⁵ mol l⁻¹; ε = 7206).

3.2.4.12. [(C₉H₇N)B₈H₁₁NH^{iso}Pr] **28**. Compound **3** reacts with chinoline to give **28**. R_F = 0.63; Yield: 53% (15 mg, 53 μmol); NMR (CDCl₃): BH(2) -54.6 [-0.46]; BH(8) -32.2 [+0.0 *endo*, *exo* +1.03]; BH(7) -29.4 [+1.03]; BH(4) -29.4 [+0.81]; BH(3) -17.0 [+2.31]; BH(5) and BH(6) both at ca. -10.6 [both at ca. +2.55/2.31]; BH(1) +2.9 [+3.07]; μH(4.5)/μH(6.7) = -1.66; C(1)H +150.0 [+9.60]; C(9) +143.1; C(3)H +142.3 [+8.51]; C(7)H +132.5 [+7.99]; C(5)H +128.9 [+7.99]; C(4) +128.8; C(6)H +128.3 [+7.79]; C(2)H +120.5 [+7.61]; C(8)H +124.7 [+9.51]; NHCH(CH₃)₂ +52.9 [+2.63]; NHCH(CH₃)₂ +21.4/+21.3 [+1.20]; NH [-1.12]; Mass spectrum: FAB (NBA): *m/z*: 283 ([M]⁺, 22%), *m/z*: 285 ([M]⁻, 15%); UV spectrum: λ_{max} = 415 nm (THF; 1.98 × 10⁻⁴ mol l⁻¹; ε = 2326).

Acknowledgements

We thank the Deutsche Forschungsgemeinschaft, the Fonds der Chemischen Industrie and the UK EPSRC for support. We are also most grateful to M.B. Hursthouse and S.J. Coles of the University of Southampton for the collection of crystallographic X-ray diffraction data for compound **18**.

References

- [1] B.M. Graybill, A.R. Pitochelli, M.F. Hawthorne, *Inorg. Chem.* 1 (1962) 626.
- [2] R. Lewin, P.G. Simpson, W.N. Lipscomb, *J. Chem. Phys.* 39 (1963) 1532.
- [3] P. MacKinnon, X.L.R. Fontaine, J.D. Kennedy, P.A. Salter, *Collect. Czech. Chem. Commun.* 61 (1996) 1773.
- [4] (a) R.E. Williams, *Inorg. Chem.* 1 (1971) 210; (b) K. Wade, *J. Chem. Soc. Chem. Commun.* (1971) 792; (c) K. Wade, *Adv. Inorg. Chem. Radiochem.* 18 (1976) 1; (d) R.E. Williams, *Adv. Inorg. Chem. Radiochem.* 18 (1976) 67.
- [5] U. Dörfler, M. Thornton-Pett, J.D. Kennedy, *J. Chem. Soc. Dalton Trans.* (1997) 2547.
- [6] U. Dörfler, C. Bauer, D. Gabel, N.P. Rath, L. Barton, J.D. Kennedy, *J. Organomet. Chem.* 614–615 (2000) 215.
- [7] U. Dörfler, J.D. Kennedy, D. Ormsby, R. Greatrex, *Inorg. Chim. Acta* 304 (2000) 268.
- [8] U. Dörfler, P.A. Salter, X.L.R. Fontaine, N.N. Greenwood, J.D. Kennedy, M. Thornton-Pett, *Collect. Czech. Chem. Commun.* 64 (1999) 947.
- [9] U. Dörfler, J.D. Kennedy, L. Barton, C.M. Collins, N.P. Rath, *J. Chem. Soc. Dalton Trans.* (1997) 707.
- [10] See, for example, together with references cited therein: C. Bauer, D. Gabel, U. Dörfler, Abstracts 2nd European Symposium on Boron Chemistry, EUROBORON 2, Dinard, France, September 2–6, 2001, Abstract no. O4; M. El-Zaria, U. Dörfler, D. Gabel, loc. cit., Abstract no. O8; D. Gabel, M. El-Zaria, U. Dörfler, loc. cit., Abstract no. O13; C. Bauer, J.D. Kennedy, M. Thornton-Pett, T. Borrmann, D. Gabel, U. Dörfler, loc. cit., Abstract no. P13; C. Bauer, U. Dörfler, D. Gabel, submitted to *Eur. J. Med. Chem.*
- [11] B.M. Graybill, M.F. Hawthorne, *J. Am. Chem. Soc.* 83 (1961) 2673.
- [12] T. Schaefer, R. Sebastian, R. Salman, *Can. J. Chem.* 59 (1981) 3026.
- [13] M.G.S. Londesborough, C. Price, M. Thornton-Pett, W. Clegg, J.D. Kennedy, *Inorg. Chem. Commun.* (1999) 298.
- [14] J.D. Kennedy, Boron, in: J. Mason (Ed.), *Multinuclear NMR* (Chapter 8), Plenum, New York and London, 1987, pp. 221–258.
- [15] W. McFarlane, *Proc. R. Soc. London Ser. A* 39 (1968) 185.
- [16] J.J.P. Stewart, *J. Comp. Aided Molec. Des.* 4 (1) (1990) 1–108.
- [17] HYPERCHEM 5.1, HyperCube Inc., Waterloo, Ontario Canada.
- [18] Z. Otwinowski, W. Minor, DENZO-SMN, Processing of X-ray Diffraction Data Collected in Oscillation Mode, *Methods Enzymol.* 276 (1997) 307–326. C.W. Carter, R.M. Sweet, (Eds.) Academic Press; COLLECT, Data Collection Strategy Program, Nonius, 1999.